High Availability Path Design in Ring-Based Optical Networks

Wayne D. Grover, *Senior Member, IEEE*

***Abstract*— This work develops mathematical models for path availability and provisioning resources required in various strategies for realizing high availability service paths in a transport environment of bidirectional line-switched rings or shared protection optical (wavelength division multiplexing) rings. The work originated in response to user requests for SONET service paths with unavailabilities under 30 s/year. A number of schemes for redundant routing and ring interconnection are considered as options to meet such a demanding target in the most economic way. An analytical framework for comparison of various provisioning schemes allows a "cost effectiveness" assessment of four high-performance alternatives, in terms of total resource investment and the corresponding service unavailability relative to a single-fed path construction. The logical models of cost and availability can be used in a variety of SONET or optical-ring transport planning studies or perhaps in future automated provisioning tools. An important finding is that while the availability benefit of dual-ring interconnection is high in metro-ring networks, the availability of paths through long-haul ring networks may be relatively poor due to lower limits from two-failure intra-ring combinations.**

I. Introduction

A. Background

MODERN society is highly dependent on the availability of communication services such as voice, data, video-conferencing, Internet, private networking, credit verification, etc. Yet all these services are multiplexed and transported on a relatively sparse backbone of high-capacity fiber-optic transmission links. The impact of failure can be drastic [1], [2]. There are currently two main approaches to provide a "self-healing" capability for these networks. These are, generically, the ring [3]–[11] and mesh [12]–[20] restoration strategies. In a self-healing mesh, demand flows are restored by agile re-routing through the relatively small allocations of spare capacity on other spans of the network. Control of the process may be distributed [12], [14]–[16], [18] or centralized [12], [19]. The relatively high-capacity efficiency of mesh-restorable networks [17], [20] tends to offset the cost of the digital cross-connect systems they use, making them effective in long-haul networks. In comparison, rings require greater total capacity but reconfigure independently in a much simpler switching reaction and are based on less expensive add-drop multiplexer (ADM) equipment [3]–[7]. Rings consequently tend to predominate in metropolitan networks today. The design and provisioning problems of both types of network are active areas of study [8], [9], [11], [13], [17], [20].

In this work, we are concerned with questions of constructing new service paths in an already deployed ring-based network. Specifically, our interest is in the availability versus cost of various schemes for provisioning redundant service paths that traverse one or more rings. Both ring and mesh restoration techniques can make a network 100% *restorable*, in the sense that for any single span failure, there are enough simultaneously feasible restoration paths in spare capacity to re-route all of the affected paths. But this does not imply 100% availability. Two sources of outage remain: 1) dual (or higher order) simultaneous failures and 2) outage during the reconfiguration time. The second of these is, however, easily disregarded: the reconfiguration delays for rings are 50–60 ms [6], [7]. Even ten reconfigurations a year would contribute only 1.5×10^{-8} toward unavailability, which is orders of magnitude less than the dual-failure outage contributors. Ring switching times are thus almost transparent to most customers and usually appear only as one errored second [12].

Another reason to study the availability of paths through networks that are already "fully restorable" is that leased line and private networking customers often have contracts with assured availability objectives. Typically, a service-level agreement may provide a free month if there is more than a minute of outage in the preceding month. However, as we will show, there are several policies that a network operator could use for high-availability path provisioning. The network operator could be over-providing the equipment redundancy (and hence cost) for the required design availability without a cost-versus-availability assessment framework. For instance, the "matched-node" *(mn)* interconnection scheme [3]–[7] seems to be a default procedure today which we think may exceed requirements in some circumstances. In others, dual feeding *(df)* with direct transfers between rings, an alternative which we propose, could be less costly for essentially the same availability.

B. Objectives, Scope, and Outline

Specifically, we aim to provide a methodology, comparative insights, and quantitative results on ring-network path-provisioning strategies. We provide a general model for the two-failure outage of transport rings due to node or link failure within the ring, for single- and *df* cases. We then provide a model of end-to-end availability for paths implemented over concatenated rings with *df* or *mn* arrangements. After

Manuscript received June 6, 1996; revised February 1, 1998; approved by IEEE/ACM TRANSACTIONS ON NETWORKING Editor K. S. Vastola.

The author is with TRLabs, Edmonton, AB, Canada T5K 2P7 (e-mail: grover@edm.trlabs.ca).

Publisher Item Identifier S 1063-6692(99)06391-8.

developing general analytical results, we apply them in a comparative study of alternative strategies in four networking environments. Standard methods and assumptions for availability analysis are used, after reviewing them below.

The remainder of Section I relates this work to prior literature. Section II introduces the two main inter-ring connection options to be considered. Section III covers the methodology and assumptions involved in the availability calculations, and explains the relative cost-assessment model. Section IV develops end-to-end path unavailability and resource cost functions for each scheme considered. These expressions can be used for a variety of other studies on single rings and chains of rings with user-specific path models, cost, and unavailability data. Section V presents a comparative study in long-haul and short-haul network scenarios. Section VI summarizes main findings.

C. Literature

The main transport rings found today are SONET-based, although the logical structures they represent could be implemented in many technologies. SONET is a set of standard formats for fiber-optic payload-multiplexing physical layer interfaces, and ring-based protection switching [22], [23]. In SONET terminology, the two types of logical transport ring are the bidirectional line-switched ring (BLSR) and the unidirectional path-switched ring (UPSR) [6], [7].[1] These are, respectively, equivalent in their logical structure and operation to the more recent wavelength division multiplexing (WDM)-based "shared protection optical ring" and "path-protected optical ring." Recently considerable emphasis has been put on the optimized design of ring-based networks [4]–[11] and on development of mesh-restoration control schemes [14]–[16], [18], [19]. The focus generally has been on achieving the property of full restorability against any single failure but without directly linking this to service availability.

To and Nuesy [24] have, however, considered the availability of SONET rings and certain digital cross-connect restoration schemes over a ladder-type hypothetical reference digital path (HRDP). They derive results for 2-fiber and 4-fiber BLSR's, but do not consider the interconnection issues in a chain of rings. Their analytical method and assumptions are, however, the same as we use. To *et al.* [25] also use these methods to compare the availability of 2-fiber and 4-fiber BLSR's. Nagaraj *et al.* [26] provide a comparative study of the impact of SONET technology on network availability relative to the preceding DS3-based transport era. They do not develop analytical results, but provide an example of the comparison of schemes on an HRDP model, with the same assumptions as To and Neusy [24]. Wilson has conducted similar comparisons of 2- and 4-fiber rings but does not compare the ring interconnection models covered here [27].

A seemingly relevant body of literature, judging by name only, would be that of "network reliability" in the sense of [28], [29], [31]. However, this field is focused on questions of topological disconnection between pairs, or sets of points, in a graph where any number of link failures may be outstanding. The two-terminal reliability [29] is the closest to our concept of a digital or light path, but assumes that if at least one route exists topologically between end points, the service will be available. This is of some relevance to idealized packet routing, but it is hard to apply to SONET or WDM transmission networking, where there are definite routing, restoration, and capacity constraints. Network reliability has no consideration of standby redundancy, and the repair of physical failures, and assumes nodes are completely reliable. The methods of network reliability also allow link-failure probabilities that are significant fractions of one, ruling out some simplifying numerical approximations that can be useful where the availability of elements is well over 99.9%. As Spragins also has argued [21], [30], [32], we need to consider the availability of specific path configurations through networks, with detailed functional consideration of the failure and reconfiguration mechanisms, not measures of the graph-theoretic extent to which a topology alone remains connected in the presence of accumulating failures. Spragins has also pioneered the treatment of dependent failure issues [35]–[37], which we also consider in our specific context.

More recently, Willebeek-LeMair and Shahabuddin [38] studied the availability of paths between stations in a FDDI LAN, which has a "wrapping mechanism" somewhat like that of the BLSR. They focus is on a single FDDI[2] ring and its associated trees of concentrators and attached stations. The authors comment on the difficulty of Markov modeling and Monte Carlo simulation for problems involving analysis of paths through multi-node networks with both link and node failures and an active reconfiguration mechanism. This is quite relevant and supportive to the approach we take. Falconer, however, has approached the modeling of a variety of single-ring LAN architectures through Markov models [40]. However, as both [33] and [38] mention, this leads to considerably greater complexity and difficulty in representing the entire state space and its transition probabilities. Our experience is similar; for modeling paths through multi-ring networks, the state–space explodes combinatorially, and yet direct enumeration of the outage-causing failure combinations is relatively accessible from a functional understanding of the structures involved.

II. Dual-Ring Interconnect Options

The two main logical ring types are the UPSR and BLSR. Documentation on these structures is widely available [6], [7], [22], [23]. Briefly, in a UPSR, two counter-rotating unidirectional rings provide redundant, geographically diverse paths for each demand pair. All nodes transmit their signals onto both rings in opposite directions. Each node thus receives two copies of the signals routed to it and simply performs $1 + 1$ receiver selection. In a BLSR, a logically or physically distinct standby ring is used on a shared basis by all nodes and spans.

[1] Bellcore has standardized the UPSR. Bellcore and ANSI T1 have standardized BLSR's and ITU has standardized the MS-SPRING, which is the SDH equivalent of the BLSR.

[2] It is interesting to note that FDDI is not logically unrelated to SONET, FDDI would occupy the role of a unidirectional line-switched (ULSR) ring, were it a SONET standard.

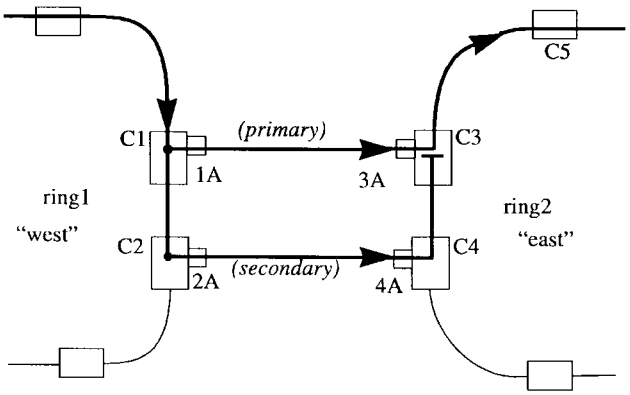

Fig. 1. *mn* drop & continue inter-ring transfer arrangement.

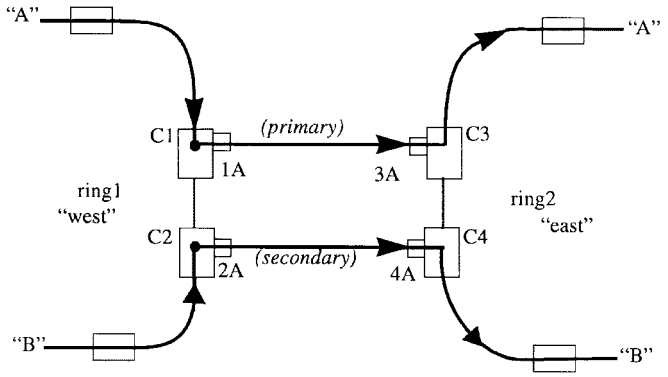

Fig. 2. *df, dt* inter-ring arrangement.

Restoration is by loopback switching to/from the bidirectional spare system at nodes adjacent to a failure. In a 4-fiber BLSR the protection ring is a physically distinct bidirectional fiber ring. In a two-fiber BLSR, a logical protection ring is formed by dividing the channels in a single physical ring into working and protection channel groups. For example, in an OC-48 BLSR/2, STS-1 channels 1–24 may form a *working* bidirectional ring and STS-1 channels 25–48 form a logical *protection* ring.

When an individual payload signal (often called a tributary, e.g., and STS-1) is in the body of a BLSR, it is protected against any single node or link failure by the reverse-direction routing mechanism. But, without special measures, there will be a single point of failure where a ring-to-ring transfers occur. This may be acceptable for some applications because the transfer occurs inside a building, and the cross-office wiring (or fibering) may itself be $1+1$ protected on its run through the building. It is often desired, however, literally to avoid any single points of failure. Thus, the *"mn"* (also called "drop and continue") arrangement (Fig. 1) is widely used [4], [5]. The service path transfers redundantly via two nodes ("matched" to each other) using the drop-and-continue arrangement. In Fig. 1, labels C1–C4 and 1A–4A designate the ADM cores and add/drop interfaces involved. A unidirectional signal flow is drawn, but a mirror image for the other direction is implied. The transferring signal enters the primary *mn* C1, where it is "dropped" to C3 and "continued" (still on ring 1) to the secondary node C2. The "drop" signal at C1 is supplied via a cross-office link to the primary gateway, C3, for a standard tributary addition into ring 2. The continue signal in ring 1 is dropped again at C2, and this time is not continued. It transfers to become an "add" signal at node C4. C3 thus receives two copies of the transferring signal. In the event of failure affecting its local add signal, it switches to the surviving copy arriving in the line signal from C4. This arrangement resists any single failure of ADM cores or add/drop interfaces involved. It also protects against a number of dual-failure combinations. A more detailed analysis follows. Henceforth we will refer to this form of dual ring interconnect as simply *mn*.

df is an alternative which we suggest. Direct transfers *(dt's)* are made at the same two crossing points, but from two explicit signal feeds in the originating rings without any drop and continue setups (Fig. 2). This may seem naive at first glance because it completely doubles line utilization in the related rings. We will show, however, that when all resources are considered, there are circumstances where *df* can be lower cost than *mn*, at essentially the same unavailability. Fig. 2 shows how the service is simply duplicated in each ring and transfers directly at each gateway node. Clearly there will be circumstances where this consumes more ring bandwidth than the *mn* setup but we will show that in some circumstances, *df* may cost less than *mn*.

III. Methodology for Estimating Availability and Resource Requirements

A. Methodology for Assessing Service Unavailability

Availability is the probability that a repairable, maintained, system will be in the operating state at any time in the future. Time includes all intervals of successful operation and elapsed time during which the system was down. *Reliability* is the probability that a system or component will operate without any failure to provide its end function or service for a specific interval of time, starting from a no-fault state [39], [42], [45]. Redundant components may be switched in, but repair of the failures is not presumed in the latter context. Thus, for example, it is *reliability* that is of concern in a space launch, but *availability* the relevant measure for a transport network service path. Further, it is the availability of specific customer path configurations, or—in a study like this—of hypothetical reference paths (HRDP) that is relevant, not the fraction of time that the entire network is operating [21]. We use a type of approximate availability analysis that is often used by network operators and manufacturers for comparative studies of alternatives. It involves the use of an HRDP [43] for comparison of alternative policies and some simplifying assumptions for availability analysis [39], [41]–[42] which are summarized here. The most common equation for availability is $A = \mathrm{MTBF}/(\mathrm{MTBF} + \mathrm{MTTR})$ where MTBF is the mean time between failures, and MTTR is the mean time to repair. Related to this is the *unavailability* of a system, or element, $U = 1 - A$. In the telecommunications industry there is an established framework for approximate availability analysis, based on the following assumptions. These are also

the premises of availability modeling in [24]–[27], [38], [39], [41]–[46].

(i) A two-state "working–failed" model describes the status of all elements.
(ii) All elements fail independently (aside from specific common-cause failure mechanisms that may be identified for consideration).
(iii) The in-service times (or times between failure) and repair times are independent memoryless processes with a constant mean.
(iv) The repair rate is very much greater than the failure rate. Equivalently, the MTTR is much smaller than the MTBF.
(v) The "most likely paths to failure" approach is used (to be described).

These assumptions are generally sufficient for comparative analysis of engineering alternatives when describing a large number of system instances, over a long time of nominal operating conditions. Regarding points (ii) and (iii), it is obviously important to take specific vulnerabilities into account in the model, such as routing supposedly separate signals through a common cable duct. Only failure of elements that appear to be independent to someone with functional knowledge of the system design and operation are assumed independent. Without assuming this independence at some level, however, one virtually cannot proceed on problems of practical importance because the set of possible multi-element failure combinations is always huge [29]. One can always postulate arbitrary common cause–failure scenarios with widespread effects (e.g., a storm, an earthquake) that are not in the model. But then there is a virtually infinite number of such scenarios and no data about the probabilities involved [29]. It is important, therefore, to proceed with reasonable assumptions so that comparative insights can at least be obtained (in our case, for input to provisioning policy formulation) under a plausible operating model. It is important, in this regard, to see this as a formalized kind of reasoning about alternatives, rather "than any kind of absolute predictor of future performance" (paraphrasing [48]). For our problem, the important dependent failure situations to identify are as follows.

Folded rings: In a "folded" ring, cable sections pertaining to logically separate arcs of a ring are installed in the same duct. This practice obviously defeats the main purpose of using a ring for restoration. Network operators usually pay attention to the physical routing of the cable segments to ensure physical diversity. Nevertheless, where only one physical right-of-way or duct is available, rings are sometimes used in a folded configuration as a point-to-point transmission system, in which the ring action functions as protection against single electronics or optics failures, but not cable cuts. Our models do not apply to "folded rings." They can, however, be easily modified to reflect folded rings by replacing the span-span and span-node dual failure combinations in the $Td1()$, $Td2()$ functions (to follow) by single common-cut or duct-failure outage probabilities.

Co-routed continue spans: Another common-cause failure consideration arises if the continue spans between *mn* rings are implemented in the same cable or duct. This particular single-cause dual-element failure *by itself* is not outage-causing. It only alters the remaining failure combinations that lead to outage from that state. Our baseline model assumes that continue signals at interfacing rings are physically independent. In developing the unavailability model for the relevant cases, however, we will indicate how to modify the expressions for this special case.

Building failure: Another consideration is that physically co-located ADM terminals may fail together if an entire building is destroyed or suffers total power loss. Such failures are far less frequent than individual electronics or cable failures, but it is important to realize that a building failure never affects more than one ADM on any ring at the same time. Many co-located ADM's may thus fail together, but effects are dispersed over separate rings. Aside from *mn* building failures, this is consequently just another contributor to the elemental unavailability of terminals in a ring, with no limitation on the analysis. Although the individual ADM failures are correlated the impact is always dispersed as single node failures in separate rings.

Point (iv) is evident from operating experience. For instance, To and Nuesy [24] give data for 100 miles of optical cable (the component of highest failure rate in practice) for which $\mathrm{MTBF} = 19\,000$ hours, $\mathrm{MTTR} = 12$ hours. Point (iv) is also the basis of a very useful simplification. It implies that $\prod_{i=1}^{n} A_i \approx 1 - \sum_{i=1}^{n} U_i$, where A_i is the availability of the ith of n elements in a series relationship, and U_i is the corresponding *unavailability*, $1 - A_i$. It says we can "add unavailability instead of multiplying availabilities" for elements or subsystems in series. Freeman [42] illustrates the typically high accuracy of this approximation with an example of six elements in series with U_i from 10^{-5} to 10^{-3}. The accuracy of the approximation is better than 0.5%, which is "typically far more precise than the estimates of element A_i's". [42, p. 2073]. A simpler way to appreciate this is to consider just two elements in series for which $A_{\text{exact}} = A^*A = (1-U)(1-U) = 1 - 2U - U^2$, which shows that the approximation $A = 1 - 2U$ omits only the square of an already small number U^2.

Point (v) is the "most likely paths to failure approach" as termed in [38]. It means we proceed by enumeration of the simplest failure combinations that, from a functional understanding of the system, are the shortest causality sequences leading to outage. System availability is approximated by summing effects of these dominant classes of failure combinations. As long as the assessment of failure combinations is combinatorially complete over single-, double-, or perhaps triple-element failure combinations, we get a good approximation to the actual outage probability, especially as elemental U's tend to zero. The reasoning is that if there is a way for two failed elements to bring down the service, this is much more likely than is even a large number of possible three-element outage scenarios. The validity of this can be seen in a simple argument for a ring of 16 spans and nodes. There are $\binom{32}{2} = 496$ double failure combinations and roughly ten times as many triple failure combinations. But, even with a high elemental U, such for the 100 miles of cable in [24], the

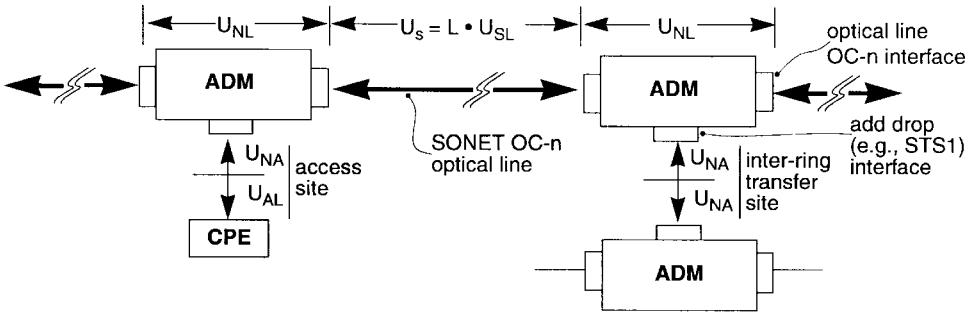

Fig. 3. Elemental unavailability and resource cost models for ring network elements.

TABLE I
ELEMENTAL UNAVAILABILITY VARIABLES

Variable	Description	Nominal Study Value
U_{SL}	Unavailability per km of ring fiber span, excluding ADM nodes and ADM optical interfaces	$5.5*10^{-6}$
U_{NL}	Unavailability of line signal path through the ADM core, without any add/drop on the signal unit.	$5.5*10^{-6}$
U_{NA}	Unavailability of add/drop interface functionality of an ADM	$5.5*10^{-6}$
U_{AL}	Unavailability of customer access link from CPE to add/drop interface, but excluding CPE and add/drop interface on ADM	$4.5*10^{-5}$

U^3 term for triple failures means that, even if all triples were outage-causing, their total contribution would be ~1000 times below the double-failure contributions. Our results are based on this kind of analysis for all single and double failures, but not triple failures.

B. Equipment Model and Elemental Unavailabilities

The elemental unavailability variables we use for ADM's and optical lines are illustrated in Fig. 3 and Table I gives values we use for these elemental sources of unavailability in later numerical results. The upper ADM's in Fig. 3 are shown as part of an OC-n ring, characterized by U_{SL} unavailability per kilometer. The left ADM is shown as an access site from customer premises equipment (CPE). The other ADM is interfacing to an ADM in another ring. The elemental unavailability $2U_{\mathrm{NA}}$ is incurred for the tributary signal to make the cross-office connection between ADM's, including the two add/drop interfaces involved. Half of the cross-office unavailability associated with each side of the transfer is built into U_{NA}. In the access link from the CPE, the add/drop interface is considered to have the same U_{NA} for a cross-office transit, plus unavailability contributed by the outside plant access link U_{AL}. U_{AL} includes its half of the cross-office interface to the first ADM in the signal path. In practice the values in Table I depend on vendor, product maturity, and cable installation practices, etc. Determination of such unavailability estimates is outlined in sources such as [39], [43], [45]. The particular values used here were provided as planning figures from a U.S. inter-exchange carrier based on their operating experience, and on data from equipment vendors. The data are fairly consistent with a few other accessible sources, such as [24]–[26], but the exact values are not of primary importance in this study. The main requirement is only that the numeric values for the later case study center the comparative calculations in the orders of magnitude found in practice. Three of the elemental values are also numerically equal for study purposes, so that a kilometer of line, an ADM core, and an ADM add/drop interface, are notionally equal contributors to failures for this comparative study. Different numerical values can of course be used in the general expressions that follow.

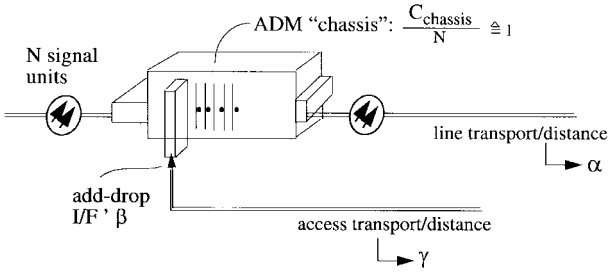

Fig. 4. Normalized cost framework for resource-consumption functions.

C. Resource Consumption Functions

For a comparative study seeking insights of a general nature we aim to avoid dependence on specific product or technology cost data. We therefore normalize various identifiable cost elements into a "resource consumption function" as a surrogate for dollar cost. The scheme for representing the relative cost of resources is in Fig. 4. Four structural characteristics are considered: 1) distance-dependent costs of the optical line; 2) ADM "core" resources; 3) add/drop interface circuit packs

used incrementally at an ADM; and 4) access link costs between the rings and the CPE or other payload source, at the start and end of the service path. The full cost of one ADM core (or "chassis"), normalized to the number of tributaries it can support, is defined as the "unit cost". For example, if STS-1s are being provisioned on an OC-48 ADM, the unit cost is $1/48$ the ADM 'core' cost. The ADM core provides all the common equipment (card cage, backplane, power supplies, control processors, and optical line interfaces) to put it in a ready-to-operate state but before any STS or wavelength λ add/drop cards are populated. β is defined as the relative cost of an add/drop interface on the ADM at the tributary rate being provisioned. α and γ are the costs of a unit distance of transmission for *intra*-ring and access transport, respectively, at the rate of the tributary being routed. This framework embodies the main economics of ring network planning as found in [4], [5], [11].

The parameters α, β, and γ of the resource cost model can be used to reflect variations in network geographic scale and different technology assumptions. For instance, in metropolitan networks, where span distances do not require regenerators, and ample dark fiber may be available in existing ducts, distance-related transmission costs are often treated as negligible [4], [5] and total cost is dominated by terminal not line equipment. In our framework, this is the $\alpha = 0$ environment. On the other hand, in a long-haul network, significant right of way, cable installation, and regenerator costs may be allocated to each fiber (or λ) used, resulting in total distance-related costs greater than the total ADM terminal costs. In this case, α^{-1} can be set to the length of installed line system which costs the same as one ADM core. For both metro and long-haul applications, β can reflect the ADM technology epoch. For instance, imagine that an STS-3c add/drop interface has a fixed (absolute) cost, but is usable for STS-3c applications on OC-48 ADM's or newer OC-192 ADM's. If the OC-192 core costs twice as much as its OC-48 predecessor, then β can reflect this difference: e.g., the core now serves four times the capacity at twice the cost, lowering the "unit cost" by a net factor of two. Since the STS3 add/drop cost is fixed, β would go up by a factor of two.

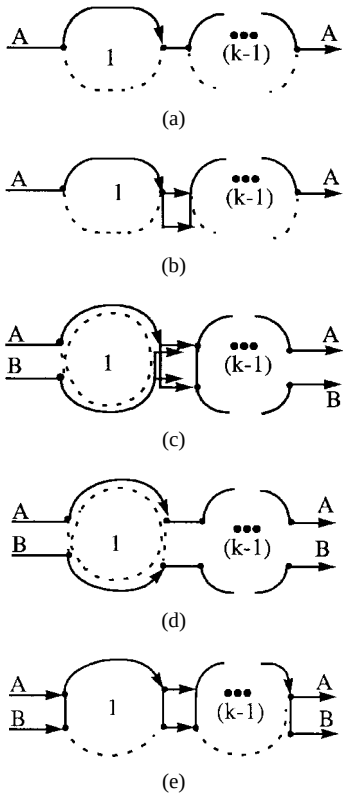

Fig. 5. Iconic sketches illustrating the principles of the five-ring network routing alternatives.

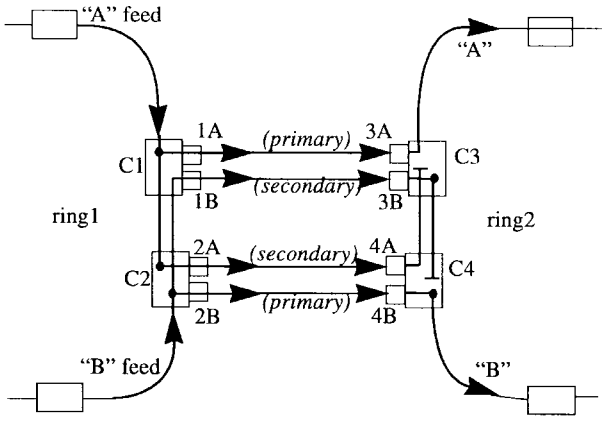

Fig. 6. *df, mn* inter-ring transfer arrangement.

IV. High-Availability Path-Provisioning Strategies

A. Path-Level Models

Having introduced the *mn* and *df* alternatives for dual-ring interconnect, we now identify four policies that could be used for constructing high-availability paths in a BLSR ring environment. Fig. 5 provides an iconic representation for four diversely provisioned path schemes plus the base-case model of the single-fed *(sf)* path. Each sketch (a)–(e) is an abstraction of where the tributary signal path being provisioned is physically present in each ring, and its mode of transfer between rings. Solid lines represent the physical presence of the service-bearing digital path or light path λ. The dotted lines complete the outline of the individual rings that the signal traverses and represent the intra-ring reverse-direction routing that the working signal path will take in the event of *intra*-ring failure affecting the signal. Between rings is a simplified representation of the *inter*-ring interface that applies. For *mn* transfers, the detail of Fig. 1 is implied by the simplified representation of the drop and continue crossings in Fig. 5(b) and (e). Similarly, the full detail for the *df, dt* scheme (d) is that of Fig. 2. The corresponding details for interface (c), *df, mn*, are in Fig. 6, which remains to be covered.

Each case in Fig. 5 represents a path which starts at, but excludes, the CPE, traverses an access link of length L_a, then enters and traverses a total of K BLSR's interconnected at $(K-1)$ *inter*-ring interfaces. Each ring is characterized by its number of spans S; the average length of spans L_s; and the number of spans traversed by the working signal path within each ring W. The signal path finally exits at the drop side of

TABLE II
NETWORK AND EQUIPMENT SCENARIOS FOR COMPARISON OF PROVISIONING STRATEGIES

Case	Description / Name	Ring Span length *Ls* (km)	Number of Spans in ring, *S*	*W* (or *Wa*)	α^{-1}	β	γLa
1	"Metro" - Large Rings	20	15	6	∞	0.8	0.25
2	"Metro" - Small Rings	20	5	2	∞	0.8	0.25
3	"Long Haul" - Large Rings	200	15	6	30	0.8	1
5	"Long Haul" - Small Rings	200	5	2	30	0.8	1

ADM's on the Kth ring, and then traverses a second access section. For clarity, signal flows are shown in one direction only but the reverse direction is always implied. The ring network hypothetical reference path parameters L_s, L_a, W, S, and the ranges we use for them, are summarized in Table II.

We now explain and analyze the five path-provisioning policies in Fig. 5. In these developments, the functions *Td*1() and *Td*2() are the dual-failure *intra*-ring unavailability of each individual ring along the service path for single and dual-feeding inside a ring, respectively. We first assume *Td*1() and *Td*2() and address the resource consumption and unavailability of each scheme on an end-to-end basis. Subsequently, expressions for *Td*1() and *Td*2() are given to complete the end-to-end mathematical models for the unavailability of each scheme.

Note that in the end-to-end unavailability models there is no explicit representation of redundancy that may be present in the "cross-office" connections at access, drop, and inter-ring transfer sites. In practice, there may be point-to-point intra-building protection arrangements for these signals as they travel floor to floor etc., within the same building. Our approach is to recognize that the presence or absence of such cross-office protection can be subsumed in the numerical value of $U_{\rm NA}$ that is used at the path-level inter-ring transfer model. This avoids the added complexity and application assumptions that would arise from explicitly modeling the cross-office protection subsystems in the end-to-end path unavailability models.

A related issue is the distinction between 2-fiber and 4-fiber BLSR's. A 4-fiber BLSR can be implemented to protect single fiber or optoelectronic element failures over the same-span in an APS-like manner if the spare is unaffected (i.e., a single regenerator failure as opposed to a cable cut) [25]. Thus, the 4-fiber BLSR has the added benefit of a subsidiary "equipment" protection switching system at the span level. The effect is that the 4-fiber BLSR can withstand certain combinations of equipment and cable-cut failures which would lead to outage in the BLSR/2. To be precise, our models are based on the functional behavior of 2-fiber rings and may thus be slightly pessimistic for 4-fiber rings. The 2-fiber/4-fiber BLSR difference is, however, an *intra-ring* issue, so the structure of the path level models that follow are unchanged, only the internal details of *Td*1() and *Td*2() functions would change. With paper length in mind, we will simply point out later the differences in the derivation of *Td*1() and *Td*2() that would describe the BLSR/4 case and proceed based on the BLSR/2 case. We do not expect, however, that the insights and conclusions reached are dependent on the 2-fiber/4-fiber distinction. Indeed, one investigator [27] has found it acceptable to model the protection switching subsystem in BLSR/4 simply as a numerical improvement in the span unavailability data used in a BLSR/2 behavioral model.

B. *sf* Path

Single-feeding [Fig. 5(a)] is the least available but lowest-cost routing strategy. It will serve as the reference case to which the effectiveness of more redundant routing schemes are compared. The *sf* path follows a shortest route from source to destination. Starting from a nonredundant customer access link, the signal is "added" at the access node on first ring and traverses W_1 spans of that ring (which has S_1 spans in total). It is then dropped from the first ring, traverses a cross-office *inter*-ring connection, is added to the second ring, and so on through a total of K rings. In the Kth ring the signal is dropped at the egress ADM node and completes its routing on a second nonredundant access link.

Aside from the cross-office inter-ring interfaces, the *sf* signal is protected by the line protection mechanism against single span or node failures *inside* any ring along its path. Certain two-failure combinations in the same ring will, however, cause outage, given by the *Td*1() function to follow. Summation of series element unavailabilities for the *sf* path leads to

$$U_{\rm sf} = 2[U_{\rm AL} + K(U_{\rm NA} + U_{\rm NL})] + \sum_{i=1}^{K} Td1(W_i, S_i). \quad (1)$$

$2U_{\rm AL}$ is from the access links. $2(U_{\rm NA} + U_{\rm NL})$ is the single-point of failure outage of the access and egress ADM's in their add/drop interfaces or in the core of the access or egress ADM nodes. Single-node ADM failures are covered by the BLSR's line protection reaction from an *intra-ring* transport viewpoint, but if the core of the access (or egress) ADM is lost, there will be outage in *sf*. $(K-1)$ pairs of similarly vulnerable drop/add interfaces occur in series between the K rings for an outage contribution of $2(K-1)(U_{\rm NA} + U_{\rm NL})$. The sum of *Td*1() terms covers the *intra*-ring unavailability due to *double* failures within each ring in the path.

The resource consumption function for *sf* is addressed by considering the quantity of ADM cores, add/drop interfaces, distance-bandwidth product on spans, and access-link consumption. (This sequence is repeated for all schemes.) Inside each ring on the *sf* service path, there are W_i working spans and W_i+1 nodes. However, the cores of the access and egress ADM's on each ring are only "half-transited" by the signal path. At all other ADM's the core is fully traversed. The total ADM core consumption is therefore $W_i + 1 - 2(1/2) = W_i$ cost units per ring. Two add/drop interfaces are also used per ring and $W_i L_s$ of span transport are used in each ring where W_i is the number of spans traversed in the ith ring and L_s is the average length of spans in a ring in the reference path model. Finally, *sf* uses two access links. The resulting resource function for *sf* routing is therefore

$$C_{\mathrm{sf}} = (1+\alpha L_s)\sum_{i=1}^{K} W_i + 2K\beta + 2\gamma L_a. \tag{2}$$

C. sf Path with mn Inter-Ring Transfers (sf, mn)

The *sf, mn* routing model is the same as *sf*, except that the signal transfers redundantly between successive BLSR's via *mn's* using the *drop and continue* arrangement from Section II. The *mn* arrangement and signal selection at the receiving primary gateway protects the inter-ring transfer against failure of any of the four ADM's performing add/drop functions. By considering the line-level BLSR re-routing of each ring simultaneously with the tributary-level selection behavior in the surviving *mn*, it can be shown that it also survives total loss of either gateway *site* (e.g., both C1 and C3 or C2 and C4), and some other dual-failure combinations. For instance, if the entire node for C1–C3 fails, the tributary shown in Fig. 1 is reverse routed in the line signal in ring 1 where node C2 substitutes it for the normal signal from C1. The secondary transfer path then conveys it to C4, which is in also loopback mode in response to loss of node C3, as is the right neighbor node of C3 in ring 2. The tributary is therefore reverse routed to the latter node in ring 2, continuing its pre-failure path.

Through similar case-by-case reasoning for all possible two-element failures in the *mn* setup (summarized in Tables III and IV), it is found that only simultaneous pairs of same-ring (e.g., C1, C2) or cross-ring (e.g., C1, C4) ADM core or add/drop interface failures defeat the *mn* arrangement. Failure of both ADM cores on one side of the gateway also leads to outage, but this is accounted for in $Td1()$ as a dual-failure *intra*-ring outage. Additionally, due to the line-level BLSR reaction, the *sf-mn* scheme survives a span failure between the primary and secondary nodes on either ring combined with a single element failure in the inter-ring interface. The result is that each inter-ring transfer in *sf-mn* contributes $2U_{\mathrm{NL}}^2 + 4U_{\mathrm{NA}}^2 + 8U_{\mathrm{NL}}U_{\mathrm{NA}}$. In *sf-mn*, the access and egress links remain nonredundant, so $2(U_{\mathrm{AL}}+U_{\mathrm{NA}}+U_{\mathrm{NL}})$ is contributed by the access/egress links and add/drop interfaces. The overall unavailability is

$$U_{\mathrm{sfmn}} = 2(U_{\mathrm{AL}}+U_{\mathrm{NA}}+U_{\mathrm{NL}}) + (K-1)\cdot\left[2U_{\mathrm{NL}}^2+4U_{\mathrm{NA}}^2+8U_{\mathrm{NA}}U_{\mathrm{NL}}\right] + \sum_{i=1}^{K} Td1(W_i, S_i). \tag{3}$$

The resource cost of *sf, mn* can be approached by considering it relative to *sf*. On a per-ring basis, the ADM core consumption goes up by $1/2$ transit at primary and secondary gateway nodes, where the continue signals now complete a transit of the core. In addition, two more add/drop interfaces are used at each *inter*-ring transfer for a total consumption of $2K + 2(K-1) = 4K-2$ add/drop interfaces. Assuming *mn's* are adjacent, span usage goes up by two spans per *mn* interface for the "continue" signals. Access links are the same as for *sf*. Thus, we have

$$C_{\mathrm{sf\,mn}} = (1+\alpha L_s)\left[\left(\sum_{i=1}^{K} W_i\right) + 2(K-1)\right] + (4K-2)\beta + 2\gamma L_a. \tag{4}$$

D. df Paths with mn Inter-Ring Transfers (df, mn)

In *df, mn* routing [Fig. 5(c)], redundant signal paths are provided to/from the CPE for access and egress and each of these signal feeds is handled like *sf, mn* for inter-ring transport. The resulting inter-ring signal flow for a pair of A and B signal feeds is detailed in Fig. 6. Clearly *df, mn* is the most complex and redundant scheme, but can be understood as the configuration resulting if diverse feeds for a service were administratively treated with *sf, mn* provisioning. In the *df, mn* path, outage results only through dual access link failures or dual add/drop failures at any interface $(U_{\mathrm{AL}}^2 + U_{\mathrm{NA}}^2)$ or from an access link combined with an access ADM core, or add/drop interface failure on the opposite access path $(2U_{\mathrm{AL}}(U_{\mathrm{NA}}+U_{\mathrm{NL}}))$. Dual ADM core failures in the same ring at an interface cause outage but are part of the $Td2()$ *intra-ring df* transport outage. No outage is caused by a dual failure in the inter- ring gateway including the span between a pair of same-ring gateway nodes. This leaves us to consider all two-element failures amongst the four ADM cores and eight add/drop interfaces in Fig. 6. The case-by-case consideration of all combinations is summarized in Table 3. Aside from dual core losses on the same ring (which are in $Td2()$), there is only one two-element failure that causes outage; diagonally opposite ADM cores. Each *df-mn* inter-ring transfer consequently contributes only $2U_{\mathrm{NL}}^2$ unavailability. Summing contributors, the overall *df, mn* service unavailability is

$$U_{\mathrm{df\,mn}} = 2[(U_{\mathrm{NA}}+U_{\mathrm{AL}})^2 + 2U_{\mathrm{NL}}(U_{\mathrm{NA}}+U_{\mathrm{AL}})] + (K-1)2U_{\mathrm{NL}}^2 + \sum_{i=1}^{K} Td2\big(W_{A_i}, S_i, E_i\big). \tag{5}$$

The summation for *intra*-ring transport is now in terms of the $Td2()$ function (to follow). W_{A_i} is the length of the A signal feed within the ith ring in the service path, S_i the number of spans in the ith ring, and E_i the total number of spans of separation between access and egress node on the A and B paths where they enter and leave the ith ring. $E_i = 2$ for adjacent *mn's*.

The resource cost for *df, mn* is obtained as follows. From Fig. 5(c), we see that the *df, mn* path pair almost circumnavigates each ring. Excluding the continue spans at ring interfaces, $(S_i - 2)$ spans are traversed in each ring. All S_i

TABLE III
DUAL-FAILURE ANALYSIS FOR *sf-mn* INTER-RING TRANSFER ARRANGEMENT

Dual-element failure enumerations (Description)	Example of failure class	Unavailability (per individual combination)	No. of combinations
1) 2 ADM cores (nodes) on the same ring	C1-C2	covered by *Td1()* function for intra-ring outage	2
2) 2 ADM cores at opposite facing ADM nodes	C1-C3	not outage-causing	2
3) cores of diagonally opposite ADMs	C1-C4	$U_{NL}{}^2$	2
4) two add/drop interfaces on different nodes of the same ring	1A-2A	$U_{NA}{}^2$	2
5) two add/drop interfaces on diagonally opposite nodes	1A-4A	$U_{NA}{}^2$	2
6) two add/drop interfaces on facing opposite nodes	1A - 3A	not outage-causing	2
7) add/drop interface at a node on ring 1 and ADM core loss at diagonally opposite node	1A - C4	$U_{NA}U_{NL}$	4
8) core loss on one ring with add/drop interface loss at other node on same ring	C1 - 2A	$U_{NA}U_{NL}$	4
9) any core loss and same-node add/drop interface	C1-1A	not outage-causing	4
10) any core loss and add/drop interface at facing node	C1 - 3A	not outage-causing	4
		Total Combinations[1] =	28

[1] : This must total 28 to prove that all two-element failures amongst the set of four ADM cores and four add/drop interfaces for the *sf-mn* inter-ring transfer arrangement case have been considered, e.g., (8 choose 2)=28.

ADM cores see either the A or B signal, but at four nodes the signal only "half transits" for a total ADM core consumption of $S_i - 2$ units. In addition, $2(1/2 + 1/2)$ ADM cores are consumed for each signal feed at each inter-ring transfer, or $4(K - 1)$ additional ADM core units in the path. Four span units and eight add/drop interfaces are also used at each interface and four access/egress links are used in total. The resultant cost function is

$$C_{\mathrm{df\,mn}} = (1 + \alpha L_s)\left[\left(\sum_{i=1}^{K}(S_i - 2)\right) + 4(K-1)\right] + (8K - 4)\beta + 4\gamma L_a. \quad (6)$$

A reasonable question is "would *df, mn* ever make practical sense?" The *inter-* and *intra*-ring portions are both doubly-redundant (two explicit signal feeds with redundant transfers for each). We do not advocate or dismiss *df, mn* but offer the following thoughts on its possible role. First, note that if nonredundant cross-office links are used, *df, mn* is not really that different in detail at inter-ring interfaces from *sf, mn* if the latter is implemented with redundant cross-office links. Thus, at least one role for *df, mn* could be to permit unprotected cross-office links, investing the redundancy in the path-level construction rather than the intra-office provisioning policy. Also note (from Tables III and IV) that four of the five failure combinations that cause outage in *sf, mn* are eliminated in *df, mn*. In this sense, *df, mn* is not wholly wasteful in its use of extra resources. Considering only the inter-ring transfer unavailability for *sf, mn* and *df, mn*, the ratio of these (*sf, mn* over *df, mn*) is $(U_{\mathrm{NL}}^2 + 2U_{\mathrm{NA}}^2 + 4U_{\mathrm{NL}}U_{\mathrm{NA}})/U_{\mathrm{NL}}^2$. If $U_{\mathrm{NA}} \approx U_{\mathrm{NL}}$, *df-mn* thus offers about a seven-fold reduction in outage at the ring interfaces. With nonprotected cross-office interfaces, (higher U_{NA}) the advantage for *df, mn* is greater. If $U_{\mathrm{NA}} = 4\ U_{\mathrm{NL}}$, *df, mn* has 49 times less inter-ring outage than *sf, mn*, etc.

E. df Paths With Direct Inter-Ring Transfers (df, dt)

df, dt's is like *df, mn* except that the A and B feeds make their way directly across the inter-ring interfaces, as in Fig. 5(d), without *mn* setups. This permits a greater number of two-failure combinations to cause outage than in *df, mn*, but it considerably reduces resource use at the inter-ring interfaces. Inside each ring *df, dt* is the same as *df, mn* in that *intra*-ring dual failure outage is accounted for by *Td2()*. As in *df, mn*, single span or ADM failures in a BLSR are isolated and do not combine end-to-end. In *df, dt*, however, a failure at any inter-ring transfer on feed "A" does combine with a failure at any other interface on the "B" path, causing outage. The two add/drop interfaces at access/egress ends of the path are

TABLE IV
DUAL-FAILURE ANALYSIS FOR *df-mn* INTER-RING TRANSFER ARRANGEMENT

Dual-element failure enumerations (Description)	Example(s) of failure class	Unavailability (per individual combination)	Total combinations in class
1) 2 ADM cores (nodes) on the same ring	C1-C2	covered by *Td2()* function for intra-ring outage	2
2) 2 ADM cores at opposite facing ADM nodes	C1-C3	not outage-causing	2
3) cores of diagonally opposite ADMs	C1-C4	U_{NL}[2]	2
4) add/drop interface on either A or B feed and core loss at *same* node as add/drop	1A-C1, 1B-C1	not outage-causing	8
5) core loss and add/drop interface loss, on either A or B feed, at other node on the *same* ring	C1 - 2A, C2 - 1B	not outage-causing[1]	8
6) any core loss and add/drop interface on either A or B feeds at the *facing* node	C1 - 3A, C2 - 4B	not outage-causing	8
7) add/drop interface (on either A or B feed) at a node on one ring and ADM core loss at *diagonally opposite* node	1A - C4, 3B - C2	not outage-causing[1]	8
8) both A and B feed add/drop interfaces on the same node fail	4B - 4A 1A - 1B	not outage-causing	8
9) add/drop interfaces on the *same feed* (A or B) at both nodes on the *same* ring	1A - 2A, 3B - 4B	not outage-causing[1]	4
10) add/drop interfaces on *different feeds*, one at each node of the *same* ring	1A - 2B 3A - 4B	not outage-causing	4
11) both add/drop interfaces on the *same feed* (A or B) between facing nodes	1A - 3A 2B - 4B	not outage-causing	4
12) add/drop interfaces on *both feeds* (A and B) between pair of *facing* nodes	1A - 3B 2B - 4A	not outage-causing	4
13) 2 add/drop interfaces on the *same* feed (A or B), at *diagonally opposite* nodes	1A - 4A 2B - 3B	not outage-causing[1]	4
14) 2 add/drop interfaces on *opposite* feeds (A or B), at *diagonally opposite* nodes	1A - 4B 2B - 3A	not outage-causing	4
		Total Combinations[2]=	66

[1] : These are failure combinations that do cause outage in the corresponding *sf-mn* case.
[2] : This must total 66 to prove that all possible two-element failures amongst the set of four ADM cores and eight add/drop interfaces have been considered, e.g., (12 choose 2) = 66.

similarly non-isolated. Thus, there are $2K$ pairs of add/drop interface points and two access links on the A signal feed, which may combine with any of the similar points on the B path, and vice versa. If failure events at "A" path interfaces are independent of those on the "B" path, the unavailability from end-to-end combinable *inter*-ring transfers and access/egress links is $(2U_{\rm AL} + 2KU_{\rm NA})^2$.

There are also some two-element combinations which must happen at the same interface to cause outage. A diagonally opposite pair of core losses, each of which is individually recoverable from an intra-ring line transport view, will nonetheless fail the tributary service if they occur on both feeds at the same interface. [This is different from dual failures of both nodes on one ring at the interface, which is also outage-causing but accounted for in *Td2*().] Similarly, a core loss in one ring, combined with a diagonally opposite add/drop interface loss at the same interface, is a localized combination that causes outage and is not accounted for in former considerations. The latter add $2U_{\rm NL}^2 + 4U_{\rm NL}U_{\rm NA}$ at each inter-ring transfer. Finally, at access and egress locations, there is another local, diagonal, failure combination to account for: that of an access core loss and opposite feed link or add/drop interface failure, contributing $2(U_{\rm NL}(U_{\rm NA} + U_{\rm AL}))$ at each end. Overall, the unavailability for *df, dt* service paths is therefore

$$U_{\rm df\,dt} = 4[U_{\rm AL} + KU_{\rm NA}]^2 + 4U_{\rm NL}(U_{\rm NA} + U_{\rm AL}) + 2(K-1) \cdot [U_{\rm NL}^2 + 2U_{\rm NL}U_{\rm NA}] + \sum_{i=1}^{K} Td2(W_{A_i}, S_i, E_i) \quad (7)$$

The resource consumption of *df, dt* is easily identified as a subset of that for *df, mn*. *df, dt* is essentially *df, mn* without any of the node and span resources for "continue" signal handling at inter-ring interfaces. Therefore, as reasoned for *df, mn*, but before adding $(K-1)$ drop and continue inter-ring interfaces, we get the resource cost function for *df, dt*

$$C_{\mathrm{df\,dt}} = (1+\alpha L_s)\sum_{i=1}^{K}(S_i - E_i) + 4K\beta + 4\gamma L_a. \quad (8)$$

F. Redundant Access (ra) to mn Path (ra, mn)

Lastly we consider provisioning of *sf* paths with *mn* arrangements, as in *sf, mn*, but at access-egress points, we propose that dual access links could be supported using the same features of the ADM that support drop and continue and tributary selection in the *mn* interfaces. The idea is to treat the access interfaces as if they were instances of only the *right-hand half* of the full *mn* arrangement in Fig. 1. *ra, mn* will then have $(K-1)$ inter-ring outage contributions that are identical to *sf, mn* and *intra*-ring unavailability given by *Td*1(). At access and egress points, however, outage will now arise only from a dual access link failure at either end $(2U_{\mathrm{AL}}^2)$, or dual add/drop interface failures at the same end $(2U_{\mathrm{NA}}^2)$, or from local cross-combinations of access link and access node failures at either end $(4U_{\mathrm{AL}}U_{\mathrm{NA}})$. In contrast to *df, dt*, each access side is isolated from combining with single failures at the other end. Combinations of one access link or node and the continue signal link between the primary and secondary access nodes, do not contribute to outage because the span between the two access nodes is covered by the BLSR reaction. Once the tributary signal gets into the line signal on this span, failure of this span is restored by reverse-direction routing around the ring, which leaves the ring in an equivalent to normal state with regards to one further access-side failure. Dual-span and span-node failures in the ring involving the span between *ra* points are outage-causing but are accounted for in *Td*1(). The resulting unavailability for the *ra, mn* scheme is

$$U_{\mathrm{ra\,mn}} = 2[(U_{\mathrm{AL}}+U_{\mathrm{NA}})^2 + 2U_{\mathrm{NL}}(U_{\mathrm{NA}}+U_{\mathrm{AL}})] + (K-1)\cdot\left[2U_{\mathrm{NL}}^2 + 4U_{\mathrm{NA}}^2 + 8U_{\mathrm{NA}}U_{\mathrm{NL}}\right] + \sum_{i=1}^{K} Td1\left(W_{A_i}, S_i\right). \quad (9)$$

For resource consumption, the *ra, mn* scheme is the same as *sf, mn* with two extra access links, two extra "half transits" of ADM cores at each access, one extra span transit at each end (for the continue signals), and two extra add/drop interfaces in total. The overall effect is that all rings have W_i+2 unit core and span resources and four add/drop interfaces consumed per ring. Hence

$$C_{\mathrm{ra\,mn}} = (1+\alpha L_s)\sum_{i=1}^{K}(W_i+2) + 4K\beta + 4\gamma L_a. \quad (10)$$

G. Dependent Failure Consideration for Adjoining Continue Spans

Here. we digress to treat a common-cause failure that is possible in all path models which employ the *mn*-interface arrangement if the continue spans for the adjoining rings (e.g., (C1-C2) and (C3-C4) in Fig. 1) are implemented in the same cable or duct. If so, both can be failed by one cut. This obviously has no effect on any of the *df*-path options, and in the *mn*-path models, there is also no immediate outage: line-level reconfiguration occurs independently in the respective rings. Moreover, the working signal path in our models remains unaltered, crossing as it did before the failure from ring 1 to ring 2 via the primary gateway C1-C3. In this state, however, we require only one further failure anywhere in the primary *mn* transfer path to cause outage so the whole combination would contribute $U_S^2(U_{\mathrm{NL}}+U_{\mathrm{NA}})$. Thus, if the relevant "facing" continue spans are co-routed and subject to a fully correlated failure, this factor should be added to the existing terms which are multiplied by $(K-1)$ in (3) and (9) above. The *sf, df-dt*, and *df-mn* models are unaltered.

H. Intra-Ring Dual-Failure Line-Level Transport Unavailability Functions *Td*1(), *Td*2()

We now develop the expressions for *Td*1(W,S) and *Td*2(W,S,E) for the unavailability of *sf* and *df* signal paths through a BLSR. This includes optical line failures at the access and egress nodes, and the ADM cores, but not the add/drop side (or tributary-level) failures at these nodes as these are already represented in the *inter*-ring and access terms of the models above. *Td*1(W_i,S_i) is the line-level intra-ring transport unavailability of a *sf* signal path traversing W_i spans of a BLSR having S_i spans in total. It accounts for all double-failure combinations with an exact functional model for the 2-fiber BLSR mechanism. *Td*1(W,S), applicable in all path constructions which use *sf* transport *within* rings, is obtained as follows: let the set of W spans and $(W+1)$ nodes in the normal path of a signal feed X be called the *forward path of* X, *For*$\{X\}$. The set of other nodes and spans in the ring is *Rev*$\{X\}$, i.e., *Rev*$\{X\} = \{\{R\} - For\{X\}\}$, where set $\{R\}$ is the complete ring. *Rev*$\{X\}$ contains $S-W$ spans. For outage of an *sf* path in a ring, it is then necessary and sufficient that one failed element (node or span) belong to *For*$\{X\}$ and the other to *Rev*$\{X\}$. The relevant failure pairs consist of: a span in *For*$\{X\}$ and a span in *Rev*$\{X\}$, a span in *For*$\{X\}$ and a node in *Rev*$\{X\}$, or vice versa, and a node in *For*$\{X\}$ and a node in *Rev*$\{X\}$. Triple failure combinations are ignored. Summing and simplifying all contributions, we obtain

$$Td1(W,S) = W(S-W)U_S^2 + (W+1)(S-W-1)U_{\mathrm{NL}}^2 + [2W(S-W-1)+S]U_S U_{\mathrm{NL}} \quad (11)$$

A slightly different function *Td*2() is needed for the intra-ring unavailability in *df, mn*, and *df, dt* strategies where redundant signal feeds are explicitly provisioned through each BLSR. For a *sf* path the forward path, plus the line-protection switching path, circumnavigates the ring, i.e., $|For\{X\}| + |Rev\{X\}| = S$. But when *df*, the relevant subsets do not comprise the whole ring together. With *df* A and B paths, outage requires one failure in $\{For\{A\}$ *AND* $Rev\{B\}\}$ and the other in $\{Rev\{A\}$ *AND* $For\{B\}\}$. This is the only way two failures can be positioned so as to simultaneously fail A and B forward feeds and both respective line-restoration

paths. However, because the normal A, B signal feeds are disjoint paths $\{Rev\{A\}\ AND\ For\{B\}\} = For\{B\}$. This is because $For\{B\}$ is necessarily a *subset* of the path $Rev\{A\}$. Likewise, $\{For\{A\}\ AND\ Rev\{B\}\} = For\{A\}$. Thus, outage requires simultaneous failures in A and B feeds, but there is no exposure to failures on spans/nodes of the ring that are not directly on one of the A/B feeding paths. For example, when a *df* path pair enter and leave the ring one node apart $|For\{A\}|+|For\{B\}| = S-2$, meaning that there are two less spans contributing to failure combinations than with *sf*. From these considerations, the dual-failure outage of a *df* path pair in a BLSR simplifies to

$$Td2(S,Wa,E) = WaWbU_S^2 + (Wa+1)(Wb+1)U_{\rm NL}^2 + (2WaWb+Wa+Wb)U_S U_{\rm NL} \qquad (12)$$

where $Wb = S - Wa - E$ and Wa is the length of the (arbitrarily designated) A path, S is the number of spans in the ring, and E is the total of the number of spans separating A and B access and egress node pairs of the *df* path pair. For fully (node and span) disjoint *df* $E_{\min} = 2$.

The above implies that *df* through a BLSR will not give the kind of intra-ring unavailability reduction that is normally expected from $1+1$ redundancy, i.e., $O(U^2)$, because the restoration path $Rev\{A\}$ for signal feed A is so highly intersected with the forward path of the B feed, and vice versa. In other words, the explicitly duplicated signal feed plays a survivability role that almost (but not wholly) overlaps with the ordinary line protection mechanism. *df* will have some availability gain, however, to the extent that the overlap of $For\{B\}$ and $Rev\{A\}$ paths (and vice versa) is not complete; i.e., the spans between the node pairs where the A/B paths enter and leave the ring, are removed as outage-contributing combinations. The greatest (intra-ring) benefit from *df* is therefore when relatively large rings are involved and the access and/or egress node pairs for the signal feeds (or both) can be widely separated on the ring.

BLSR/4 $Td1(), Td2()$ models: For the 2-fiber BLSR, a single working-fiber failure (also called an "equipment" failure [24]) and a cable cut both cause ring protection switching. $Td1(), Td2()$ can be modified, however, to reflect that a 4-fiber BLSR can handle single "equipment" failures without using the protection ring, by subtracting a term for the expected outage from this type of failure in the expressions just given. To do this, the single U_s value describing a span has also to be decomposed into $U_s = U_{\rm sc} + U_{\rm se}$ to resolve cable cut span unavailability $U_{\rm sc}$ from single-fiber affecting transmitter/receiver or electronics outage $U_{\rm se}$. The compensating terms are $-W(S-W)U_{\rm se}^2$ for (11) and $-WaWbU_{\rm se}^2$ for (12). The 2-/4-fiber availability difference is discussed further in [24].

Applicability to UPSR: Although we specifically treat BLSR's in this work, it is worth noting that, as also observed in [27], the $Td1(), Td2()$ functions are equally applicable to UPSR's. Although UPSR and BLSR mechanisms differ, the fundamental arguments that service outage requires one failed element in $For\{X\}$ and another in $Rev\{X\}$) are equally governing for the UPSR. Consequently, to the extent that chains of UPSR's may be interconnected with functional arrangements equivalent to *mn's* or *dt's*, the path level unavailability models may be the same or only slightly different in UPSR reference path models, although these details remain to be worked through. The BLSR resource cost models would, however, not apply directly to UPSR cases.

V. Application Study

A. Framework for Results

We now use the models above to compare service unavailability and resource consumption for hypothetical reference path models which reflect various network scenarios through $\{L, S, W, \alpha, \beta\}$ parameter sets. The purpose is to gain comparative insights about the efficacy of the various provisioning strategies in different networking scenarios. The baseline in each case will be the *sf* path; the minimum option for provisioning any new service. The four other schemes will be compared in terms of unavailability and resource consumption relative to *sf* for the same length of service path. The *relative* unavailability and cost are denoted U_R, C_R, respectively. K will be the number of rings in the service path. Normalization to the *sf* path provides a framework for cost-benefit assessment of the high availability schemes, viewing them in a C_R versus U_R plane. In this framework, the *sf* path will always be at the point $(U_R, C_R) = (1,1)$. The comparative insights from this approach should be true over a range of reasonable numeric values for the elemental unavailability and cost data.

B. Network Scenarios

The parameters defining various network scenarios are given in Table II. The "metro" cases reflect a short (nonrepeated) 20-km span length (L_s) and negligible line-related transmission costs α, (i.e., an "infinite" span length equals the cost of the ADM core). There is no conflict in having a finite span length L_s but virtually no cost for line transmission because L_s is a contributor to the unavailability, even if it has no cost. "Long haul" cases have $L_s = 200$-km reflecting span distances in inter-exchange carrier networks. The long-haul spans are costed so that the average installed OC-n span cost equals one ADM core cost at about 30 km. Across these basic scenarios of geographic scale, we overlay two extremes of logical "ring size," referring to the number of spans in each ring S, and to W (or Wa), which is the number of spans traversed in each ring by the shortest path routing of the service. The "large rings" case assumes $S = 15$ and W (or Wa) $= 6$. "Small rings" assumes $S = 5$ and W (or Wa) $= 2$. For *df, dt* and *df, mn*, which involve dual A and B signal feeds inside each ring, Wa denotes the shortest of the two paths in a ring and equals W in the *sf* schemes. Wb is then a dependent variable $(Wb = S-Wa-E)$. For *df, dt*, E is the total number of spans separating "A" and "B" feeds at their access and egress node pairs on each ring. We use $E = 2$ for basic comparisons of *df* against *mn* schemes based on inputs that multi-span "continue" signal configurations are strongly avoided. *df, dt* can, however, have any E value in $2 < E < (S-Wa-1)$ as resulting from the pair of signal feed entry/egress locations chosen. Therefore,

TABLE III

Dual-element failure enumerations (Description)	Example of failure class	Unavailability (per individual combination)	No. of combinations
1) 2 ADM cores (nodes) on the same ring	C1-C2	covered by *Td1()* function for intra-ring outage	2
2) 2 ADM cores at opposite facing ADM nodes	C1-C3	not outage-causing	2
3) cores of diagonally opposite ADMs	C1-C4	$U_{NL}{}^2$	2
4) two add/drop interfaces on different nodes of the same ring	1A-2A	$U_{NA}{}^2$	2
5) two add/drop interfaces on diagonally opposite nodes	1A-4A	$U_{NA}{}^2$	2
6) two add/drop interfaces on facing opposite nodes	1A - 3A	not outage-causing	2
7) add/drop interface at a node on ring 1 and ADM core loss at diagonally opposite node	1A - C4	$U_{NA}U_{NL}$	4
8) core loss on one ring with add/drop interface loss at other node on same ring	C1 - 2A	$U_{NA}U_{NL}$	4
9) any core loss and same-node add/drop interface	C1-1A	not outage-causing	4
10) any core loss and add/drop interface at facing node	C1 - 3A	not outage-causing	4
		Total Combinations[1] =	28

in our results we present *df, dt* at both $E = 2$ and $E = 6$ when ring size permits, so that *df, mn* and *df, dt* are in one case compared without special advantage for *df, dt*, and in the other, we get an upper estimate for the benefit of high E cases in *df, dt*.

The last two columns of Table III detail the relative cost of an add/drop interface β and the relative cost of the access link γL_a. To simplify results, we treat the product γL_a as a single parameter. The value of $\beta = 0.8$ is used for all test cases based on cost data obtained for an OC-48 ADM and STS-3c add/drop interfaces. β is kept constant to imply use of the same equipment, while only the routing strategies and network scenarios vary. The relative cost for an access link in "metro" cases $\gamma L_a = 0.25$ modeling a 5-km access link over facilities whose bandwidth pro-rated cost would equal the corresponding cost portion of the ADM core at 20 km (e.g., $\gamma = 0.05$/km). The same type of access facility, but four-times longer, is assumed in the long-haul cases.

C. Results for "Metro-Large Rings" Scenario

Fig. 7 plots the unavailability and resource costs for *sf, mn, df, mn, df, dt*, and *ra, mn* routing schemes, relative to the *sf* path option, with K running from 1 to 20 rings, under the "large rings-metro" scenario. *sf, mn* exhibits the lowest relative cost and, as expected, is identical to *sf* for $K = 1$. The relative cost of *sf, mn* rises and levels off at about 1.4 as K increases. The relative availability of *sf, mn* improves as path length increases but, even at $K = 20$ ($U_{R,\mathrm{sf\,mn}} = 0.23$) there only a 4.3 times reduction in unavailability over the *sf* option.

In contrast *ra, mn*, which is *sf, mn* with *ra*, is much more effective. $C_{R,\mathrm{ra,mn}}$ ranges narrowly between 1.5 and 1.475 from $K = 1$ to 20, similar to *sf, mn* at the longer path lengths. When the *ra, mn* path is long enough to amortize the extra access costs relative to *sf, mn*, it begins to have a relative cost similar to *sf, mn*. However, *ra, mn* does much better in unavailability due to the access redundancy. By implication from the results, the access link is the limiting factor to the availability with *sf, mn*. Providing *mn* inter-ring transfers is therefore of little end-to-end benefit if the access and egress arrangements are not already redundant. In contrast to *sf, mn, ra, mn* also has its best U_R at short path lengths; being 143 times less unavailable than *sf* at $K = 1$ and 38 times better at $K = 20$.

Above *ra, mn* in Fig. 7 we find the loci of *df, dt* $(E = 6)$, *df, dt* $(E = 2)$, and *df, mn* schemes. With $S = 15$ in this case, values of $E = 2$ and $E = 6$ are chosen for *df, dt* to bracket the probable extent of the total entry/egress separation in real circumstances. Fig. 7 shows that the most effective scheme would be either *ra, mn* or *df, dt* if "wide egress" can be achieved for the latter. If not, *df, dt* (at $E = 2$) and *df, mn* are both unattractive in these circumstances. The relative cost (C_R) for *df, dt* (at $E = 2$) is roughly 50% higher than

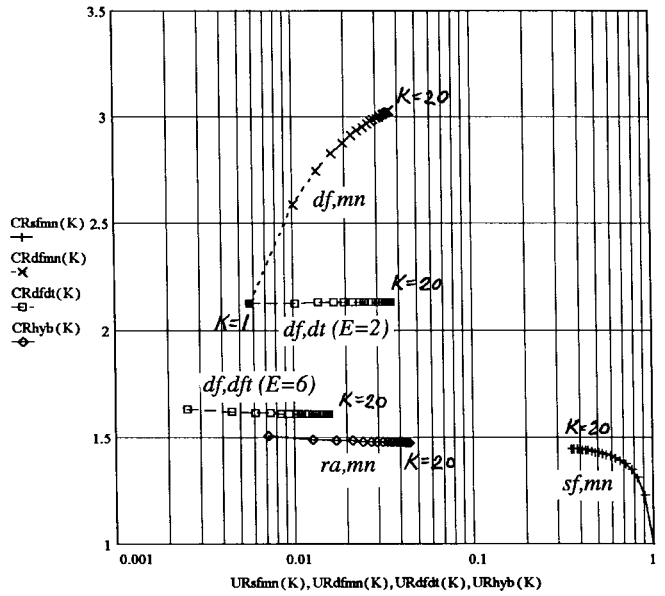

Fig. 7. Results for "metro-large rings" network test case.

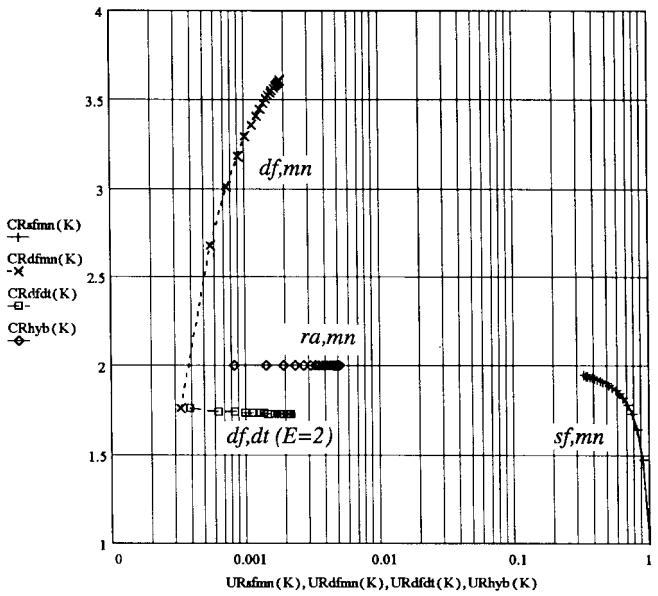

Fig. 8. Results for "metro-small rings" test case.

ra, mn but offers only ∼25% lower unavailability. *df, mn* has even higher costs despite being without any further U_R benefit relative to *df, dt* (at $E = 2$).

The absolute *intra-ring* unavailabilities explain a great deal about the results in Fig. 7. In the metro large-ring scenario, *Td*$2(6, 15, 2)$ is 5.69×10^{-7} (17.8 s outage per year per ring). For schemes which use *sf* *Td*$1(6, 15) = 7.13 \times 10^{-7}$ (about 22.3 s per ring per year). By comparison, the relevant terms in (3) and (7) show that *mn* and *dt* styles of *inter-ring* transfers and access outage contributions are both 10–100 times below these *intra-ring* values, on a per-instance basis. This explains why *ra, mn* is the most effective scheme in Fig. 7 (if *df, dt* is not granted $E = 6$): *ra, mn* is the least equipment-intensive scheme which provides at least some form of redundancy over all portions of the path. *df, dt* and *df, mn* offer lower levels of *inter-ring* unavailability, but those improvements are masked by the larger *intra-ring* outage expectations and the fact that even with *df* the *intra-ring* outage is not significantly lower than for *sf*. In general, therefore, when rings are large, *ra, mn* is a good contender by virtue of providing at least some form of redundant transfer and access, while achieving almost the same *intra*-ring performance as *df*, but without the cost of a second explicit intra-ring feed. The only competitor to *ra, mn* is *df, dt* if circumstances permit high E.

D. "Metro-Small Ring" Case

Fig. 8 corresponds to Fig. 7, but for smaller ring sizes $(S = 5)$ and smaller intra-ring path lengths $(W = 2)$. Given $S = 5$, we consider only $E = 2$ for the *df, dt* case. Fig. 8 shows *df, dt* is now the clear winner. Note also that the U_R for all three schemes *ra, mn*, *df, dt*, and *df, mn* are reduced roughly an order of magnitude over Fig. 7, although the costs *relative* to *sf* have also all increased. Notably, however, the U_R values are 300–2300 times reduction in unavailability relative to *sf*. These large improvements are attributable in these circumstances to the greater importance of *inter-ring* unavailability in the small rings scenario. Small rings and short path lengths make for considerably smaller *Td*$1()$ and *Td*$2()$ *intra-ring* outages, which allows the differences in *inter*-ring interface strategy to make a greater difference between schemes. We now have *Td*$1(2, 5) = 7.7 \times 10^{-8}$ and *Td*$2(2, 5, 2) = 2.9 \times 10^{-8}$. Not only are these *intra*-ring unavailabilities much smaller than above, they differ far more between themselves than in the large rings. The higher relative costs arises because the cost of paths through the smaller rings are dominated more by ring interfacing costs than in the large ring cases.

Part of the reason *df, dt* wins so clearly in Fig. 8 is also explained as a simple topological effect. In a ring of five spans, with $W = 2$, the continue spans for *ra, mn* require four span units for a total of six span signal units and the equivalent of four full ADM core traversals per ring. By comparison, *df, dt* with $Wa = 2$ and $S = 5$ implies $Wb = 1$, in which case only four units of span resource, and the equivalent of three full core traversals arise in total. So, in suitably small rings, an explicitly "*df*" path can actually require *fewer* of *all* intra-ring resources than the corresponding *mn* path. Similar considerations explain why the U_R of *df, dt* is better than *ra, mn* in the small rings: *Td*$2(2, 5, 2)$ is 2.7 times lower than *Td*$1(2, 5)$. This is because the *df, dt* path is now dependent on significantly fewer intra-ring elements than *ra, mn*. *ra, mn* depends on the integrity of all spans in the ring $(S = 5)$. But in *df, dt* the dependency is limited to the $Wa + Wb = 3$ spans in the small rings; only three out of the five spans are involved in *df, dt* failure combinations. Now compare that to the $S = 15$ case with $Wa = 6$ and $E = 2$. In that case, $Wa + Wb = S - 2 = 13$ spans (out of 15) are involved in the *df, dt* outage combinations. We expect, therefore, a much bigger difference between *df, dt* and *ra, mn* intra ring outages in small rings as compared to larger rings.

In general, we can expect *df, dt* and *ra, mn* to compete with each other depending on the exact network and costing circum-

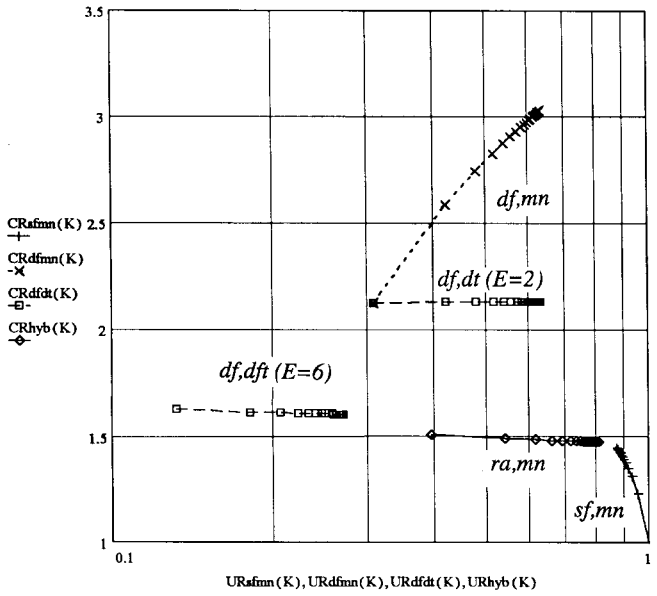

Fig. 9. Results for "long-haul large rings" test case.

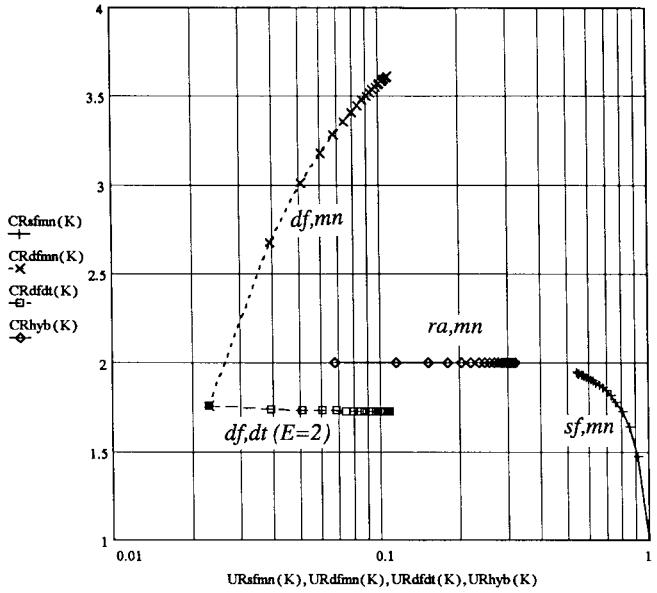

Fig. 10. Results for "long-haul small rings" test case.

stances, with interplay from all the effects just discussed. From these principles, however, *ra, mn* will generally tend to have the advantage in large rings, and where span-related costs are significant. On the other hand, *df, dt* will tend to outperform *ra, mn* when rings are logically small (i.e., few spans), when wide access/egress path pair separation is achieved, and/or when there is cost dominance by the add/drop interfaces, as opposed to span transmission costs.

E. "Long-Haul" Cases

The results in Figs. 9 and 10 parallel those of Figs. 7 and 8, respectively, but with "long haul" parameters $L_s = 200$ km, $\alpha^{-1} = 30$ km, and $\gamma L_a = 1$. Fig. 9 shows that in the long-haul large-ring circumstances, *df, dt* will be far the most cost effective scheme if wide egress applies. Otherwise *ra, mn* is the lowest cost of the high availability schemes, although at a little higher U_R. Most significantly, however, we see that there is very little U_R benefit to be had by *any* scheme: no alternative achieves even a ten-fold improvement over *sf*. This results from the *intra*-ring outage functions *Td*1() and *Td*2() rising, respectively, to 6.6×10^{-5} and 5.1×10^{-5} in response to the 200-km span unavailability of $U_{\rm SL} * L_S = 1.1 \times 10^{-3}$. At these levels of *intra*-ring dual-failure unavailability, there is little effect or benefit from variations in the ring interfacing technique (as long as some form of redundant transfer is used). The differences in U_R that are seen are solely attributable to *Td*1() and *Td*2() intra-ring outage differences. If wide egress is attainable for *df, dt*, U_R improves by reduction of the set of relevant span failure combinations in *Td*2(), but is still less than ten times better than the *sf* baseline. We see here that when the *intra*-ring unavailabilities dominate (due to long spans), it is difficult to achieve major reductions in service unavailability by investing in path diversity within the same rings. This is especially true for longer paths. For example, the best U_R in Fig. 9, at $K = 6$, is *df, dt* with the benefit of $E = 6$ which represents only a four-fold unavailability reduction over *sf*. To do better than this in long-haul rings, one may have to consider seeking *df* routes over physically *distinct rings*, e.g., "A" and "B" service feeds do not appear anywhere in the *same* rings en-route. In general, however, there is little assurance that a ring-distinct pair of signal routes exists for any one arbitrarily chosen demand pair in a typical ring-based network. Fig. 10 is the "small ring" long-haul counterpart to Fig. 9. The range of availability enhancement is improved noticeably relative to Fig. 9, to factors of about 18 at $K = 6$ for *df, mn* and *df, dt*. This is, however, also a modest improvement given the investment in redundancy that either requires. As in the metro, small rings case, however, *df, dt* again costs significantly less and offers better availability than *ra, mn*, for the reasons already discussed.

VI. Concluding Discussion

This work provides a framework for cost-availability comparison of five possible schemes for provisioning service paths through a series of dual-interconnected transport rings. In all scenarios considered, *df, dt* or *ra, mn* provided the lowest cost at the lowest or near-lowest unavailability. The choice of *ra, mn* or *df, dt* depends on the ring size, path length in the rings, and the relative costs in a way that would require each set of circumstances to be tested in detail using the methods in this paper. The tendency, however, will be for *ra, mn* to be preferred in large rings and when distance-related costs are important. The advantage in cost and unavailability will tend to be for *df, dt* in smaller rings, when inter-ring add/drop costs dominate over span distance costs, and when widely separated ring access and egress node pairs can be arranged between the A/B feeds (the "high E" case). Wherever the *df* path permits $E > 2$, *df, dt* should be considered. An unquantified further benefit when *df, dt* proves in is that

the complexity of establishing and operating *mn* interfaces is also avoided.

A possibly important general observation is that if the per kilometer unavailability of fiber is around the value used in this study (5.5×10^{-6}) then *long-haul* ring network availability may be dominated by dual intra-ring failures. Even with *df* there is little intra-ring outage improvement relative to an *sf* path with the normal *intra*-ring protection. *df* can, however, be economically advantageous in small rings, or when E is high, by eliminating continue-span resources. Thus, *df, dt* should be seen primarily as a tactic to make *inter-ring* transfers less costly, not to obtain any significant unavailability improvement from *df*.

A next step would be to consider making *df* and *mn* policy choices on a ring-by-ring basis along a multi-ring service path. The two basic approaches for ring interconnection (*mn* and *df*) are compatible with each other at inter-ring transfer points; i.e., a *df, dt* egress signal pair become the "add" inputs to an *mn* pair in the next ring, which may operate in *ra, mn* routing mode, and vice versa. A mechanized planning system of the future could consider each ring along a service path and recommend either *df, dt* or *ra, mn* for best cost-performance on the path as a whole. It could also compute the resulting end-to-end service unavailability over the mixed *ra, mn*/*df, dt* path and identify the rings with greatest contribution to path cost and unavailability. At the time of final revisions, the latter work has been completed in the form of a companion paper to this one [49].

ACKNOWLEDGMENT

Parts of this work developed out of a project with Dr. G. Brown of *BTLabs*. During that work, the *Td*1() function and a precursor of the *Td*2() functions were first derived.

REFERENCES

[1] W. E. Falconer, "Service assurance in modern telecommunication networks," *IEEE Commun. Mag.*, pp. 32–39, June 1990.
[2] J. C. MacDonald, "Public network integrity—Avoiding a crisis of trust," *IEEE J. Select. Areas Commun.*, vol. 12, pp. 5–12, Jan. 1994.
[3] T. H. Wu, *Fiber Network Service Survivability*. Norwood, MA: Artech House, 1992.
[4] T. Flanagan, "Fiber network survivability," *IEEE Commun. Mag.*, vol. 28, pp. 46–53, June 1990.
[5] Nortel (Northern Telecom). (1996). *Introduction to SONET Networking* [Online]. Available HTTP: http://www.nortel.com/broadband
[6] GR-1400-Core, *SONET Dual-Fed Unidirectional Path Switched Ring (UPSR) Equipment Generic Criteria*, Bellcore, Issue 1, Revision 1, Oct. 1995.
[7] GR-1230-Core, *SONET Bidirectional Line-Switched Ring Equipment Generic Criteria*, Bellcore, Issue 2, Nov. 1995.
[8] O. J. Wasem, T.-H. Wu, and R. H. Cardwell, "Survivable SONET networks—Design methodology," *IEEE J. Select. Areas Commun.*, vol. 12, pp. 205–212, Jan. 1994.
[9] T.-H. Wu and R. H. Cardwell, "A multi-period design model for survivable network architecture selection for SONET interoffice networks," *IEEE Trans. Rel.*, vol. 40, pp. 417–427, Oct. 1991.
[10] T.-H. Wu, D. Kong, and R. C. Lau, "A broadband virtual path SONET/ATM self-healing ring architectures and its economic feasibility study," *IEEE J. Select. Areas Commun.*, vol. 9, pp. 834–840, Dec. 1992.
[11] W. D. Grover, J. B. Slevinsky, and M. H. MacGregor, "Optimized design of ring-based survivable networks," *Can. J. Elect. Comput. Eng.*, vol. 20, no. 3, 1995.
[12] J. Sosnosky, "Service applications for SONET DCS distributed restoration," *IEEE J. Select. Areas Commun.*, vol. 12, pp. 59–68, Jan. 1994.
[13] A. Gersht, S. Kheradpir, and A. Shulman, "Dynamic bandwidth allocation and path-restoration in SONET self-healing networks," *IEEE Trans. Rel.*, vol. 45, pp. 321–331, June 1996.
[14] S. Hasegawa, Y. Okanoue, T. Egawa, and H. Sakauchi, "Control algorithms for SONET integrated self-healing networks," *IEEE J. Select. Areas Commun.*, vol. 12, pp. 111–119, Jan. 1994.
[15] W. D. Grover, "Method and apparatus for self-healing and self-provisioning networks," U.S. Patent 4 956 835, Sept. 11, 1990.
[16] W. D. Grover, B. D. Venables, M. H. MacGregor, and J. H. Sandham, "Development and performance verification of a distributed asynchronous protocol for real-time network restoration," *IEEE J. Select. Areas Commun.*, vol. 9, pp. 112–125, Jan. 1991.
[17] R. R. Iraschko, M. H. MacGregor, and W. D. Grover, "Optimal capacity placement for path restoration in mesh survivable networks," in *Proc. IEEE ICC'96*, pp. 1 568–1 574.
[18] W. D. Grover, "Distributed restoration of the transport network," *Telecommunications Network Management into the 21st Century—Techniques, Standards, Technologies, and Applications*, S. Aidarous and T. Plevyak (Eds.). Piscataway, NJ: IEEE Press, ch. 11, pp. 337–419, 1994.
[19] C. W. Chao, P. M. Dollard, J. E. Weythman, L. T. Nguyen, and H. Eslambolchi, "FASTAR-A robust system for fast DS3 restoration," in *Proc. IEEE GLOBECOM'91*, pp. 39.1.1–39.1.5.
[20] M. Herzberg and S. Bye, "An optimal spare-capacity assignment model for survivable networks with hop limits," in *Proc. IEEE GLOBECOM'94*, pp. 1601–1607.
[21] J. D. Spragins, J. C. Sinclair, Y. J. Kang, and H. Jafari, "Current telecommunication network reliability models: A critical assessment," *IEEE J. Select. Areas Commun.*, vol. SAC-4, pp. 1168–1173, Oct. 1986.
[22] B. Allen, "SONET," in *The Electronics Handbook*, J. C. Whitaker (Ed.). Boca Raton, FL: CRC, 1996, ch. 100, pp. 1524–1537.
[23] C. A. Siller and M. Shafi (Eds.), *SONET/SDH: A Sourcebook of Synchronous Networking*. Piscataway, NJ: IEEE Press, 1996, pp. 211–217.
[24] M. To and P. Neusy, "Unavailability analysis of long-haul networks," *IEEE J. Select. Areas Commun.*, vol. 12, pp. 100–109, Jan. 1994.
[25] M. To, J. McEachern, and G. Copley, "Unavailability analysis of 2 vs. 4-fiber bi-directional rings," Tech. Rep. T1X1.5/91-159, Oct. 1991.
[26] K. Nagaraj, J. Gruber, J. Leeson, and B. Fleury, "Improvements in availability and error performance of SONET compared to asynchronous transport systems," in *SONET/SDH: A Sourcebook of Synchronous Networking*, C. A. Siller and M. Shafi (Eds.). Piscataway, NJ: IEEE Press, 1996, pp. 211–217.
[27] M. R. Wilson, "The quantitative impact of network survivability on service availabilities," in *Proc. 12th Ann. National Fiber Optics Engineers Conference*, Denver, CO, Sept. 1996, pp. 919–930.
[28] S. Rai and D. Agrawal (Eds.), *Distributed Computing Network Reliability*. Piscataway, NJ: IEEE Press, 1990.
[29] D. D. Harms, M. Kraetzl, C. J. Colbourn, and J. S. Devitt, *Network Reliability*. Boca Raton, FL: CRC Press, 1995.
[30] J. D. Spragins, "Telecommunication network reliability models based on network structures," in *Proc. Telecommunication Systems, Modeling, and Analysis Conference*, Nashville, TN, Feb. 1993, pp. 79–90.
[31] C. J. Colbourn, *The Combinatorics of Network Reliability*. Oxford, U.K.: Oxford University Press, 1987.
[32] J. D. Spragins, J. D. Markov, M. W. Doss, S. A. Mitchell, and D. C. Squire, "Communication network availability predictions based on measurement data," *IEEE Trans. Comm.*, vol. COM-29, pp. 1482–1491, Oct. 1981.
[33] M. Raman, J. D. Spragins, and J. L. Hammond, "Critical design considerations for rapidly reconfiguring computer communication networks," in *Proc. 19th IEEE Southeastern Symp. System Theory*, Clemson, SC, Mar. 1987, pp. 246–250.
[34] J. D. Spragins, "Token ring reliability models," in *Proc. IEEE INFOCOM'92*, pp. 934–942.
[35] J. D. Spragins, "A fast algorithm for computing availability in networks with dependent failures," in *Proc. IEEE INFOCOM'84*, San Francisco, CA, pp. 36–42.
[36] S. N. Pan and J. D. Spragins, "Dependent failure reliability models for tactical communications networks," in *Proc. IEEE ICC'83*, Boston, MA, pp. 765–771.
[37] D. R. Shier and J. D. Spragins, "Exact and approximate dependent failure reliability models for telecommunications networks," in *Proc. IEEE INFOCOM'85*, Washington, DC, pp. 200–205.
[38] M. Willebeek-LeMair and P. Shahabuddin, "Approximating dependability measures of computer networks: An FDDI case study," *IEEE/ACM Trans. Networking*, vol. 5, pp. 311–327, Apr. 1997.
[39] R. Billinton and R. N. Allan, *Reliability Evaluation of Engineering Systems: Concepts and Techniques*, 2nd ed. New York: Plenum, 1992.

[40] R. M. Falconer, "A study of techniques for enhancing the reliability of ring local area networks (LAN's)," *Ring Technology Local Area Networks*, I. N. Dallas and E. B. Spratt (Eds.). Amsterdam, The Netherlands: Elsevier, 1984, pp. 169–196.
[41] J. Fennick, *Quality Measures and the Design of Telecommunication Systems*. Norwood, MA: Artech, 1988, pp. 298–300.
[42] R. L. Freeman, *Telecommunication System Engineering*, 3rd ed. New York: Wiley, 1996, pp. 444–447.
[43] R. L. Freeman, *Reference Manual for Telecommunication System Engineering*, 2nd ed. New York: Wiley, 1993, ch. 26, pp. 2045–2077.
[44] J. E. Flood (Ed.), *Telecommunication Networks*. Stevenage, U.K.: Peregrinus, 1977, pp. 277–279.
[45] P. D. T. O'Connor, *Practical Reliability Engineering*, 3rd ed. New York: Wiley, 1991, ch. 5.
[46] P. Cochrane and D. J. T. Heatley (Eds.), *Modeling Future Telecommunications Systems*. London, U.K.: Chapman & Hall, 1996, pp. 169–171.
[47] C. L. Hwang, F. A. Tillman, and M. H. Lee, "System-reliability evaluation techniques for complex/large systems—A review," *IEEE Trans. Rel.*, vol. R-30, pp. 416–423, Dec. 1981.
[48] C. J. Colbourn, "Network reliability: Numbers or insight?," *Ann. Oper. Res.*, vol. 33, pp. 87–93, 1991.
[49] W. D. Grover, "Resource management for fault tolerant path structures in ring-based networks," *J. Network Syst. Management*. New York: Plenum Press, vol. 7, no. 4, 1999.

Wayne Grover (S'74–M'76–SM'90) received the B.Eng. degree from Carleton University, Ottawa, Ontario, Canada, the M.Sc. degree from the University of Essex, U.K., and the Ph.D. degree from the University of Alberta, Edmonton, all in electrical engineering.

He was with BNR of Ottawa and Edmonton, as a member of scientific staff and management for ten years before joining the senior management of TRLabs, Edmonton, Alberta, Canada, in 1986. Here, he is currently Chief Scientist of Network Systems, and was instrumental in the development of TRLabs from a start-up to the over 100-person level. He is also a Professor of Electrical and Computer Engineering, University of Alberta. He has authored more than 100 journal and conference publications and holds patents on 23 topics. He is a P.Eng. in the Province of Alberta.

Dr. Grover served as Associate Editor for IEEE TRANSACTIONS ON CIRCUITS AND SYSTEMS during 1995. In 1996, he received the TRLabs Technology Commercialization Award for the licensing of restoration-related technologies to industry. He is also the recipient of the 1996/97 McCalla Research Professorship in Engineering. In 1999, he received the IEEE Baker Prize Paper Award, the IEEE Canada Outstanding Engineer Award, and the Martha Cook-Piper Research Prize from the University of Alberta.